DYNAMICAL ANALYSIS OF TRANSMISSION LINE CABLES THROUGH NONLINEAR MODELS

Nilson Barbieri
Pontifícia Universidade Católica do Paraná – PUCPR & Centro Federal de Educação Tecnológica do Paraná - CEFETPR
nilson.barbieri@pucpr.br

Renato Barbieri
Pontifícia Universidade Católica do Paraná – PUCPR – Rua Imaculada Conceição, 1155 – CEP: 80215-901 – Curitiba - PR
renato.barbieri@pucpr.br

Oswaldo Honorato de Souza Júnior
Centro Federal de Educação Tecnológica do Paraná - CEFETPR
oswaldo@lactec.org.br

Abstract. *In this work the authors use linear and nonlinear mathematical models for simulation of the dynamical behavior of transmission lines cables. The numerical models are obtained through the Finite Element Method. For validation of the mathematical models, the simulated results are compared with experimental data obtained in an automated testing system for overhead line cables. Three sample lengths were used: 13, 32 and 65 meters and two load situations with 10700 and 15860N. The forced response is obtained through an impulsive excitation (impact hammer) or electromechanical shaker and the vibration signals are collected through accelerometers placed along the half sample. The eigenbehavior is analyzed using the first mode shapes and the Irvine parameter.*

Keywords*: cable, dynamical analysis, nonlinear model, Irvine parameter*

1. Introduction

Jiang et al. (2000) presented an interesting static cable analysis. A small cable segment is modeled using the symmetry properties of model and solid finite elements (brick). In this analysis the axial, torsion, flexure and contact strength are naturally coupled.

The comparative results with this formulation and the results obtained by Costello (1997) and the experimental results of Uting and Jones (1999) show great agreement for loading and unloading situations.

In despite of the results of Jiang et al. (2000), contain good information about deformations, the coupling tensions and the contact tensions, the analysis was restricted for static problems and with symmetrical loadings. The restraints applied to obtain the symmetry terms are very complex and the number of degrees of freedom of the model also is very great. These inconvenient still limit the use of this approach for the dynamic problems and long cables (even for statics analysis).

Nawrocki and Labrosse (2000) they also analyze the static behavior of cables using the method of the finite elements. In your formulation each one of the wires is discretized with geometry similar to independent *helical springs*. Although they are introduced just results for static analysis, this element also coupling the axial force, torsion and flexure. The shown results do not introduce the same confidence order with the experimental results performed in Jiang et al. (2000). However, it has the advantage of being an element with less degrees of freedom, what it enables your application for dynamic analyses and with more complex loadings.

In the dynamic analyses, an interesting approach is to introduced by Zhang et al. (2000) which includes the effect of the non-linearities of the axial deformation and the coupling of the tension and torsion, although it do not introduce numeric results with this coupling.

Similar analysis was performed by Desai et al. (1995) with quadratic finite elements in the study of galloping in transmission lines. The numeric results of this work also were obtained without the effect of the coupling tension/torsion.

Formulations that include the effect of the coupling axial/torsional was studied with details by McConnell and Zemke (1982). These authors developed theoretical models taking in consideration the coupling axial/torsional for electrics conductors ACSR (Aluminium Conductor Steel Reinforced). The experimental results that illustrate this work show proximity very good with your mathematical model and that the tension and torsion are strongly coupled. Approximate equations for the calculation of each one of the components of the constitutive matrix also were obtained by McConnel and Zemke (1982) using the experimental data and the external diameter of the cable. In this same line of modeling, McConnell and Chang (1986) showed that the vertical motion induce torsion in the cable, even in the airflow absence.

Another interesting work with respect to the axial/torsional coupling was performed by Raoof and Kraincanic (1995). Are deduced mathematical expressions of the components of the constitutive matrices for the contact cases with total sliding and without relative sliding between the cable components.

Yu and Xu (1999) and Xu and Yu (1999) analyze the dynamic behavior of cables with oil dampers. In the first of these papers is introduced the nonlinear formulation and all mathematical manipulation to reduce the equations system for just two points (the interest points for comparison with the measurements). The differentials equations, although nonlinear, also are very similar to those mentioned previously. The interesting results appear with clearness in the second paper where are introduced the stability analyses (with and without damper) and the phenomena of internal resonance.

According to Xu and Yu (1999) an important parameter for the study of the dynamic behavior of cables is the parameter introduced by Irvine (1981) and your value gives indicative of the appearance of the internal resonances. This parameter (cable sag parameter), λ^2, it is defined as being the reason between elastic stiffness of the cable and the stiffness of catenary. This parameter is vastly used in the analysis of Johson et al. (2003) and Srinil et al. (2003).

Barbieri et al. (2004a,b) analyzed the dynamic behavior of transmission line cables through linear mathematical models and with parameter identification techniques whose main goal was the identification of the structural damping.

In this work, the authors extend the analyses modelling the cables with nonlinear theories. The numeric and experimental results are compared for the linear and nonlinear systems.

2. Nonlinear formulation

Even for geometrically non-linear problems with large displacements the equilibrium conditions between internal and external forces have to be satisfied. If the displacements are approximated with the conventional displacement finite element approach by a finite number of nodal values, $\mathbf{q}$, and the equilibrium equations is obtained using the principle of the virtual works.

If $\Psi(\mathbf{q})$ represents the sum of the internal and external generalized forces, this equilibrium can be expressed as being, Zienckiewcz and Taylor (1991):

$$\Psi(\mathbf{q}) = \int_V \mathbf{B}^t \boldsymbol{\sigma} dV - \mathbf{f} = 0 \tag{1}$$

where the matrix $\mathbf{B}$ is defined from the strain definition as;

$$d\boldsymbol{\varepsilon} = \mathbf{B}\, d\mathbf{q} \tag{2}$$

$\mathbf{f}$ is the external force vector and $\boldsymbol{\sigma}$ is the stress tensor.

For geometrically non-linear large displacements the matrix $\mathbf{B}$ can be write in the form,

$$\mathbf{B} = \mathbf{B}_0 + \mathbf{B}_L(\mathbf{q}) \tag{3}$$

where $\mathbf{B}_0$ is the characteristic matrix for small displacements (it does not depend on $\mathbf{q}$) and $\mathbf{B}_L$ depends on the displacement $\mathbf{q}$.

Like the system defined in Eq.(1) it is nonlinear for large displacements, the solution of this problem type is iterative. These iterative solutions usually associate the increment $d\mathbf{q}$ with the increment $d\Psi(\mathbf{q})$ and the procedure to obtain the relation between these increments is shown in sequence.

Taking the variation of $\Psi(\mathbf{q})$ with respect to $d\mathbf{q}$ results:

$$d\Psi(\mathbf{q}) = \int_V d\mathbf{B}^t \boldsymbol{\sigma} dV + \int_V \mathbf{B}^t d\boldsymbol{\sigma} dV = \mathbf{K}_t d\mathbf{q} \tag{4}$$

where $\mathbf{K}_t$ is the *tangential stiffness matrix*.

If the deformations are relatively small, the tensions and deformations are related of the following form:

$$\boldsymbol{\sigma} = \mathbf{D}(\boldsymbol{\varepsilon} - \boldsymbol{\varepsilon}_0) + \boldsymbol{\sigma}_0 \tag{5}$$

where $\mathbf{D}$ is the constitutive matrix and the pair $(\boldsymbol{\varepsilon}_0, \boldsymbol{\sigma}_0)$ are the initial stress and strain. This way,

$$d\boldsymbol{\sigma} = \mathbf{D}\, d\boldsymbol{\varepsilon} = \mathbf{D}\mathbf{B}\, d\mathbf{q} \tag{6}$$

As $\mathbf{B}_0$ it does not depend on $\mathbf{q}$, so

$$d\mathbf{B} = d\mathbf{B}_L(\mathbf{q}) \tag{7}$$

and the expression (4) it can be write in the form:

$$d\Psi(\mathbf{q}) = \int_V d\mathbf{B}_L^t \boldsymbol{\sigma} dV + \int_V \mathbf{B}^t \mathbf{D} \mathbf{B}\, d\mathbf{q}\, dV = \int_V d\mathbf{B}_L^t \boldsymbol{\sigma} dV + \mathbf{K}\, d\mathbf{q} \tag{8}$$

where

$$\mathbf{K} = \int_V \mathbf{B}^t \mathbf{D} \mathbf{B}\, dV = \mathbf{K}_0 + \mathbf{K}_L \tag{9}$$

where $\mathbf{K}_0$ is the usual stiffness matrix for small displacements and $\mathbf{K}_L$ is the matrix associated to large displacements and depends on **q.** $\mathbf{K}_L$ is variously known as the *initial displacement matrix*, *large displacement matrix*, etc.

The expressions developed for these two matrices are:

$$\mathbf{K}_0 = \int_V \mathbf{B}_0^t \mathbf{D} \mathbf{B}_0\, dV \tag{10}$$

and

$$\mathbf{K}_L = \int_V (\mathbf{B}_0^t \mathbf{D} \mathbf{B}_L + \mathbf{B}_L^t \mathbf{D} \mathbf{B}_L + \mathbf{B}_L^t \mathbf{D} \mathbf{B}_0)\, dV \tag{11}$$

The first term in Eq. (4) can be written as being

$$\mathbf{K}_\sigma d\mathbf{q} = \int_V d\mathbf{B}_L^t\, \sigma\, dV \tag{12}$$

and is detailed in Zienckiewcz and Taylor (1991). The $\mathbf{K}_\sigma$ matrix is known as the *initial stress matrix* or *geometric matrix*.

Using the definitions of the stiffness matrix for small displacements, $\mathbf{K}_0$; the initial displacement matrix, $\mathbf{K}_L$; the initial stress matrix or geometric matrix, $\mathbf{K}_\sigma$, the Eq. (4) can be expressed as:

$$d\Psi(\mathbf{q}) = [\mathbf{K}_0 + \mathbf{K}_L + \mathbf{K}_\sigma] d\mathbf{q} = \mathbf{K}_t d\mathbf{q} \tag{13}$$

2.1. Dynamic analysis in time domain

The times integration method used in this work is described by Krysl et al. (2000). These authors show the Newmark method for nonlinear problems including Newton-Raphson's method to obtain the equilibrium for each instant time. The proposed algorithm is shown in Tab.1.

In Tab.1 (**u**,**v**,**a**) represents the displacement , velocity and acceleration vectors; {**f**} is the force vector ; {**R**} is the vector of the force residues and ε_F is the convergence tolerance for each load increment.

To include the damping matrix, [**C**], is enough to change the calculation of the effective stiffness matrix, [**K**]* and the residue vector, {**R**}. For the current iteration, i, these values corrected with the damping are calculated of the following form:

$$[\mathbf{K}]^{*(i)} = \frac{1}{\beta \Delta t^2}[\mathbf{M}] + \frac{\gamma}{\beta \Delta t}[\mathbf{C}] + [\mathbf{K}]^{(i)} \tag{14}$$

$$\{\mathbf{R}\}^{(i)} = [\mathbf{M}]\mathbf{a}_{t+\Delta t}^{(i)} + [\mathbf{C}]\mathbf{v}_{t+\Delta t}^{(i)} - \{\mathbf{f}\}_{t+\Delta t}^{ext(i)} + \{\mathbf{f}\}_{t+\Delta t}^{int(i)} \tag{15}$$

Table 1 –Newmark algorithmic equations for nonlinear problems

$i \leftarrow 0$ $\mathbf{u}_{t+\Delta t}^{(i)} = \mathbf{u}_t$ $\mathbf{a}_{t+\Delta t}^{(i)} = -\frac{1}{\beta \Delta t}\mathbf{v}_t + (1-\frac{1}{2\beta})\mathbf{a}_t$ $\mathbf{v}_{t+\Delta t}^{(i)} = \mathbf{v}_t + \Delta t[(1-\gamma)\mathbf{a}_t + \gamma \mathbf{a}_{t+\Delta t}^{(i)})]$	Predictor
$i \leftarrow i+1$	next iteration
$[\mathbf{K}]^{*(i)} = \frac{1}{\beta \Delta t^2}[\mathbf{M}] + [\mathbf{K}]^{(i)}$	effective stiffness
$\{\mathbf{R}\}^{(i)} = [\mathbf{M}]\mathbf{a}_{t+\Delta t}^{(i)} - \{\mathbf{f}\}_{t+\Delta t}^{ext(i)} + \{\mathbf{f}\}_{t+\Delta t}^{int(i)}$	residual
$[\mathbf{K}]^{*(i)} \Delta \mathbf{u}^{(i)} = \{\mathbf{R}\}^{(i)}$	displ. increment
$\mathbf{u}_{t+\Delta t}^{(i)} = \mathbf{u}_{t+\Delta t}^{(i-1)} + \Delta \mathbf{u}^{(i)}$ $\mathbf{v}_{t+\Delta t}^{(i)} = \mathbf{v}_{t+\Delta t}^{(i-1)} + \frac{\gamma}{\beta \Delta t}\Delta \mathbf{u}^{(i)}$ $\mathbf{a}_{t+\Delta t}^{(i)} = \mathbf{a}_{t+\Delta t}^{(i-1)} + \frac{1}{\beta \Delta t^2}\Delta \mathbf{u}^{(i)}$	Corrector
If : $\left\|\{\mathbf{R}\}^{(i)}\right\| > \varepsilon_F$ repeat for next iteration. $\left\|\{\mathbf{R}\}^{(i)}\right\| < \varepsilon_F$, $t \leftarrow t + \Delta t$ and go to the top.	convergence analysis

2.2. Nondimensional Irvine parameter

The nondimensional independent parameter λ^2 (Irvine, 1981) used in dynamical analysis of elastic cables with large sag is called Irvine parameter (*nondimensional Irvine parameter* or *nondimensional sag parameter*). Figure 1 shows the geometrical data and the physical parameters to define the Irvine parameter:

$$\lambda^2 = \left(\frac{\rho g L \cos\theta}{H}\right)^2 \frac{EAL}{HL_e} \tag{16}$$

where ρ is the cable mass per unit length, g is the acceleration of gravity, H is the component of cable tension in the longitudinal x-direction, L is the length of the cable , A is the cross sectional area, E is the Young's modulus of the cable and L_e is the static (stretched) length of the cable. For horizontal cables;

$$L_e \cong L\left[1 + \frac{1}{8}\left(\frac{\rho g L \cos\theta}{H}\right)^2\right] \tag{17}$$

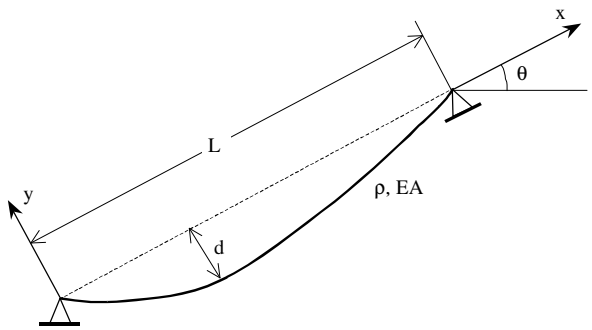

Figure 1. Inclined cable with static profile.

Internal resonance are characterized by (perfect) tuning of system natural frequencies, a situation being nearly realized for inclined cables in the so-called avoidance regions of natural frequencies ω/π, which occur for well established values of the system elastic-geometrical parameter λ/π.

The importance of internal resonance conditions occurring in multi-degree-of-freedom (MDOF) systems when the natural frequencies are commensurable with each other has been highlighted. Internal resonance cause strong modal coupling effects and result in multi-mode and multi-frequency responses. In addition, they may cause mode transition phenomena where the cable vibrates, e.g. in a purely free planar dynamics, with two companion modes which interact and combine with each other in a hybrid mode during time evolution.

3. Results

The cable used was the Ibis type whose parameters are: specific mass 0,8127 [kg/m]; rigidity flexural (EI) 11,07 Nm^2.

For the modal identification were placed five accelerometers in the cable, in the positions L/2, 3L/8, L/4, L/8 and L/16. The excitation of the system was applied through an impact hammer. The sample lengths for the mechanical load of 10700 N are: 13,385, 32,3 and 65,355m and for the load of 15860 N are: 13.395m, 32,322m and 65,378m.

The numerical results presented in this work are performed using homogeneous meshes with 80 cubic finite element and the authors developed all the computational routines.

Figure 2 (a) shows the in plane comparative results between experimental and simulated numerical linear and nonlinear approaches. Significant differences are observed in the first natural frequency. The linear model presents a significative difference (12.25%) from experimental and nonlinear model due to axial and vertical displacement coupling. Can be noticed in Fig. 2(b) that this difference are reduced with the increase load (axial cable load).

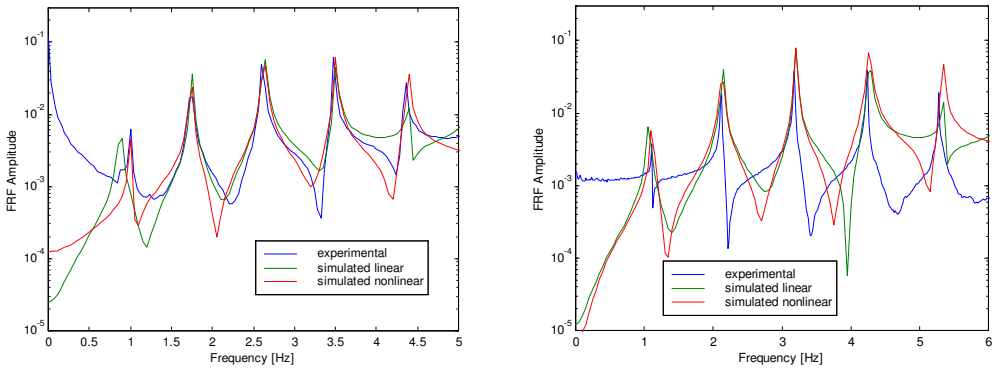

(a) (b)

Figure 2. Comparitve results for linear and nonlinear models ((a)L = 65.355 m, T = 10700 N; (b) L = 65.395 m, T = 15860 N)

In Fig. 3 the in plane FEM frequency spectrum for horizontal cables is exemplified for the first three avoidance regions $(\lambda \approx 2n\pi,\ n = 1,2,3)$. It can be noted that each avoided crossing (or veering) region can be easily identified by nondimensional Irvine's parameter $\lambda^*=\lambda/\pi$, equal to 2n with n=1,2,3...The out-of-plane frequencies are independent of the system parameter λ/π.

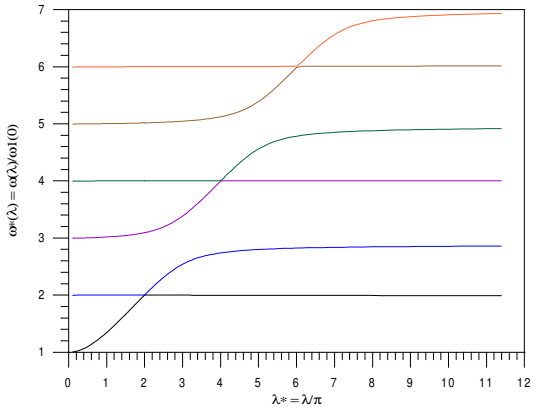

Figure 3. Natural frequency around the first three avoidance regions for horizontal cable.

The first and second vibration mode shapes are represented in Fig. 4 for the avoidance region identified by $\lambda^*=\lambda/\pi=2$.

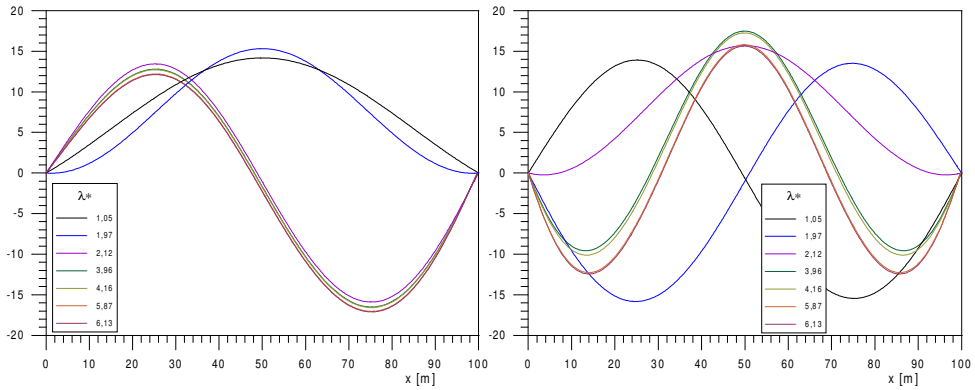

(a) (b)

Figure 4. Mode shapes: (a) first and (b) second.

Figure 5 shows the first natural frequency and first symmetric mode shape transitions around the and first avoidance region.

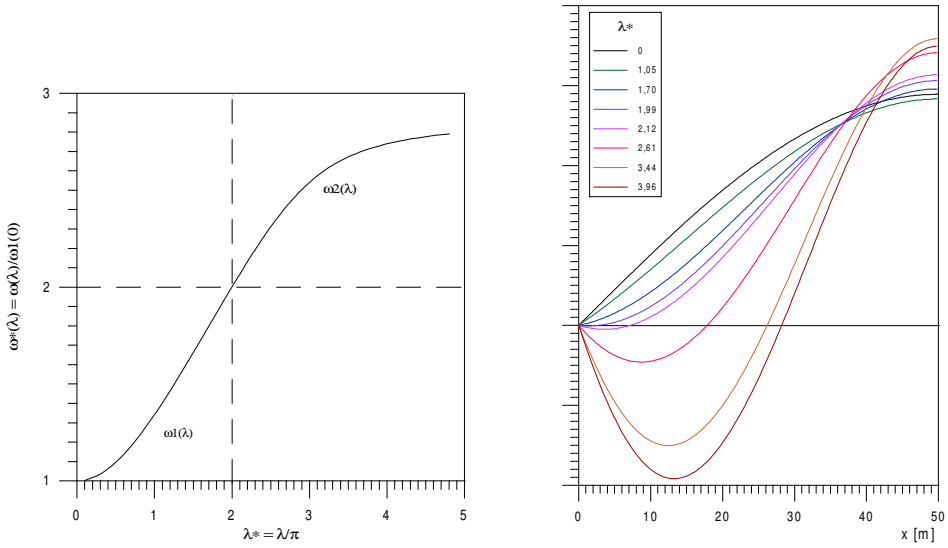

(a) (b)

Figure 5. First avoidance region for non-inclined cable: (a) frequency and (b) symmetric first mode shape transitions.

When the cable is inclined, the behavior of ω^* as function of λ^* is different. Figure 6 shows the first avoidance region and the first asymmetric mode shape for inclined cable with $\theta=30^o$. Each avoided crossing region, two in-plane frequencies became nearly close, but never equal, to each other, and the corresponding modes becomes hybrid due to a mixture of symmetric/anti-symmetric modal shapes.

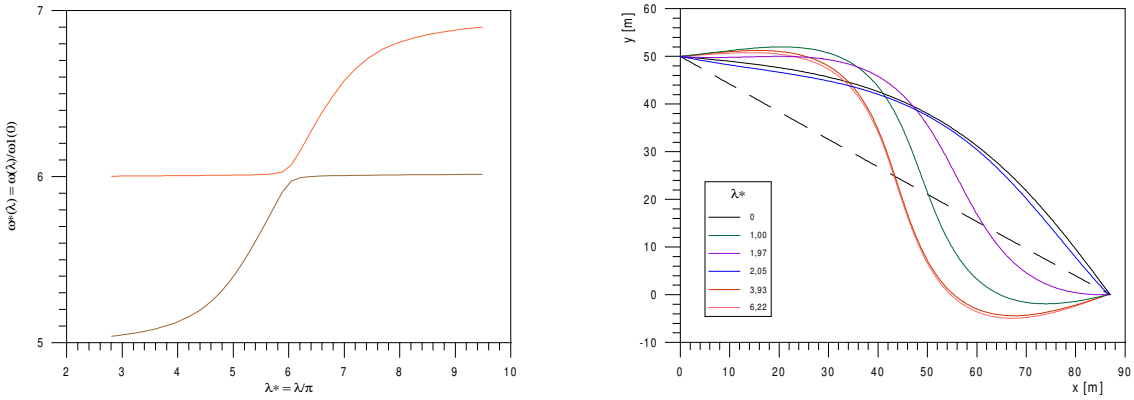

(a) (b)

Figure 6. First avoidance region for inclined cable: (a) frequency and (b) asymmetric first mode shape transitions.

Figure 7 shows the experimental and simulated results of the first mode shape in function of the Irvine parameter, for a horizontal sample test with 30.92 meters. The cable type is aluminum alloy (CAL) with 19 wires and specific mass 0.4348 [kg/m]. The test was conduced varying the cable tension and consequently the sag. The excitation was obtained through the impact hammer and the data was collected using an accelerometer.

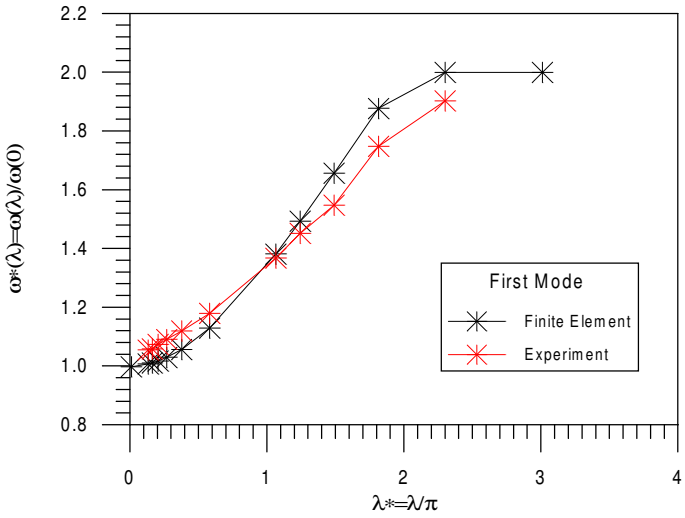

Figure 7. Experimental and numerical results of first mode shape varying the sag cable.

4. Conclusions

The nonlinear characteristics of the large amplitude free vibrations of non-inclined and inclined sagged elastic cables have been investigated numerically and experimentally.

In cables with larger sag, can be noted variations in the first natural frequencies comparing the linear and nonlinear numerical results. These variations depend on the sag and the applied load.

Strong in-plane modal coupling phenomena are observed for cables with Irvine parameter near to avoided crossing points.

The Irvine parameter can be used to detect the avoidance regions of natural frequencies. All the numeric results of this work showed good approach with the experimental results, even next to the crossing regions.

5. References

Barbieri, N., Souza Jr., O. H. and Barbieri, R., 2004a, "Dynamical analysis of transmission line cables. Parte 1- Linear Theory". Mechanical Systems and Signal Processing, Vol. 18 , n. 3 , pp. 659-669 .

Barbieri, N., Souza Jr., O. H.; Barbieri, R., 2004b. "Dynamical analysis of transmission line cables. Parte 2- Damping estimation". Mechanical Systems and Signal Processing, Vol. 18, n. 3, pp. 671-681.

Costello, G. A., 1997, "Theory of wire rope", 2nd ed. New York:Springer.

Desai, Y.M., Yu, P., Popplewell, N. and Shah, A H., 1995, "Finite element modeling of transmission line galloping". Computers & Structures, Vol. 57, n. 3, pp. 407-420.

Henghold, W. M. and Russell, J. J., 1976, "Equilibrium and Natural Frequencies of Cable structures (A Nonlinear Finite Element Approach)". Computer & Structures, Vol. 6, pp. 267-271.

Irvine, H. M., 1981, "Cable structures". Cambridge, MA: MIT Press.

Jiang, W. G., Henshall, J. L. and Walton, J. M., 2000, "A concise finite element model for three-layered straight wire rope strand". International Journal of Mechanical Sciences, Vol. 42, pp. 63-86.

Johnson, E. A., Christenson, R. E. and Spencer Jr., B. F., 2003, "Semiactive damping of cables with sag". Computer-Aided Civil and Infrastructure Engineering, Vol. 18, pp. 132-146.

Krysl, P., Lall, S. and Marsden, J. E., 2000, "Dimensional model reduction in non-linear finite element dynamics of solids and structures". Int. J. Numer. Meth. Engng, pp. 1-29.

McConnell, K. G. and Chang, C. –N., 1986, "A study of the axial-torsional coupling effect on a sagged transmission line". Experimental Mechanics, Vol. 26, pp. 324-329.

McConnell,K. G. and Zemke, W.P., 1982, "A model to predict the coupled axial torsion properties of ACSR Electrical Conductors". Experimental Mechanics, Vol. 22, n. 7, pp. 237-244.

Nawrocki, A. and Labrosse, M., 2000, "A finite element model for simple straight wire rope strands". Computers and Structures, Vol. 77, pp. 345-359.

Raoof, M. and Kraincanic, I., 1995, "Simple derivation of the stiffness matrix for axial/torsional coupling of spiral strands". Computers & Structures, Vol. 55, n. 4, pp. 589-600.

Srinil, N., Rega, G. and Chucheepskul, S., 2003, "Large amplitude three-dimensional vibrations of inclined sagged elastic cables". Nonlinear Dynamics, Vol. 33, pp. 129-154.

Uting, W. S. and Jones, N., 1999, "Axial-torsional interactions and wire deformations in 19-wire spiral strand". Journal of Strain Analysis for Engineering Design, Vol. 23, n. 2, pp. 79-86.

Xu ,Y. L. and Yu, Z., 1999, "Non-Linear Vibration of Cable-Damper Systems. Part II: Application and Verification". Journal of Sound And Vibration, Vol. 255, n. 3, pp. 465-481.

Yu, Z. and Xu, Y. L., 1999, "Non-linear vibration of cable-damper systems. Part I: Formulation". Journal of Sound and Vibration, Vol. 225, n. 3, pp. 447-463.

Zhang, Q., Popplewell, N. and Shah, A. H., 2000, "Galloping of bundle conductor". Journal of Sound and Vibration, Vol. 234, n. 1, pp. 115-134.

Zienckiewcz, O. C. and Taylor, R. L., 1991, "The Finite Element Method", 4th ed, Vol.2. Mc Graw Hill Book Company.

6. Responsibility notice

The authors are the only responsible for the printed material included in this paper.